

Holographic Bound of Casimir Effect in General Dimensions

Rong-Xin Miao *

School of Physics and Astronomy, Sun Yat-Sen University, 2 Daxue Road, Zhuhai 519082, China

Abstract

Recently, it has been proposed that holography imposes a universal lower bound on the Casimir effect for 3d BCFTs. This paper generalizes the discussions to higher dimensions. We find Einstein gravity, DGP gravity, and Gauss-Bonnet gravity sets a universal lower bound of the strip Casimir effect in general dimensions. We verify the holographic bound by free theories and $O(N)$ models in the ϵ expansions. We also derive the holographic bound of the Casimir effect for a wedge and confirm free theories obey it. It implies holography sets a lower bound of the Casimir effect for general boundary shapes, not limited to the strip. Finally, we briefly comment on the impact of mass and various generalizations and applications of our results.

*Email: miaorx@mail.sysu.edu.cn

Contents

1	Introduction	1
2	Holography I: DGP gravity	3
2.1	General discussions	4
2.2	Analytical results	9
3	Holography II: GB gravity	10
4	Holography III: GB-DGP gravity	13
5	Tests of holographic bound	15
6	Holographic bound for wedge	17
7	Conclusions and Discussions	20
A	Ghost-free condition for GB-DGP gravity	22
B	Displacement operator for GB-DGP gravity	24

1 Introduction

With the maturity of experimental techniques and potential applications in nanotechnology [1, 2, 3], the Casimir effect [4] has attracted increasing attention [5, 6, 7]. The Casimir effect also assumes a crucial theoretical significance in cosmology [9], QCD [10], and worm-hole physics [11, 12]. By definition, Casimir energy is the lowest energy of a quantum system with a boundary. Since energy should be bounded from the below, the Casimir effect is expected to have a fundamental lower bound. Inspired by the Kovtun-Son-Starinets (KSS) bound [13], [14] proposes that holography imposes a lower bound of the Casimir effect. The holographic bound passes the tests of free BCFTs, Ising model and $O(N)$ models with $N = 2, 3$ in three dimensions. Notably, unlike the KSS bound depending on the holographic models [17, 18, 19],

holography set a universal lower bound for Casimir effect [14]. The initial work [14] mainly focuses on 3d BCFTs. We generalize the discussions to higher dimensions in this paper.

Let us consider the Casimir effect of a strip in a d -dimensional flat space

$$\langle T^i_j \rangle_{\text{strip}} = \frac{\kappa_1}{L^d} \text{diag}\left(1, -(d-1), 1, \dots, 1\right), \quad (1)$$

where κ_1 is the dimensionless Casimir amplitude, and L is the strip width. Note that we impose the same boundary conditions on the two plates. Following [14], we propose the Casimir amplitude ratio to the norm of displacement operator has a lower bound in general dimensions

$$\left(\frac{-\kappa_1}{C_D}\right) \geq \frac{-2^{d-2} d \pi^{d-\frac{1}{2}} \Gamma\left(\frac{d-1}{2}\right) \Gamma\left(\frac{1}{d}\right)^d}{\Gamma(d+2) \left(d\Gamma\left(\frac{1}{2} + \frac{1}{d}\right)\right)^d}. \quad (2)$$

The displacement operator $D(y)$ describes the violation of space translation invariance normal to the boundary [20]

$$\nabla_i T^{ij} = \delta(x) D(y) n^j, \quad (3)$$

and has a positive norm $C_D \geq 0$ defined by the two-point function [20]

$$\langle D(y) D(0) \rangle = \frac{C_D}{|y|^{2d}}. \quad (4)$$

A quick way to derive the holographic bound (2) is by using Einstein gravity with the minimal tension $T \rightarrow -(d-1)$, where the corresponding κ_1 and C_D can be found in [21]. In this paper, we investigate the holographic lower bound (2) and verify its universality by studying Dvali-Gabadadze-Porrati (DGP) gravity [22], Gauss-Bonnet (GB) gravity and GB-DGP gravity. We test it with free theories and the $O(N)$ model in the ϵ expansions. See Table. 1 for a glance for 3d and 4d BCFTs. We remark that the ratios $(-\kappa_1/C_D)$ coincide for $d = 2$ and approach zero for $d \rightarrow \infty$ for all BCFTs. See Fig. 6 for example.

Table 1: $(-\kappa_1/C_D)$ for various 3d and 4d BCFTs

	Scalar	Fermion	Maxwell	Holography
3d	$\frac{-\pi\zeta(3)}{2} \approx -1.89$	$\frac{-3\pi\zeta(3)}{8} \approx -1.42$	\times	$\frac{-\pi^{5/2}\Gamma(\frac{1}{3})^3}{108\Gamma(\frac{5}{6})^3} \approx -2.17$
4d	$\frac{-\pi^6}{720} \approx -1.34$	$\frac{-7\pi^6}{8640} \approx -0.78$	$\frac{-\pi^6}{4320} \approx -0.22$	$-\frac{\pi^4\Gamma(\frac{5}{4})^4}{15\Gamma(\frac{3}{4})^4} \approx -1.94$

We also investigate the holographic bound of the Casimir effect for a wedge, which is the simplest generalization of a strip. The wedge Casimir effect takes the following form in a ground state

$$\langle T^i_j \rangle_{\text{wedge}} = \frac{f(\Omega)}{r^d} \text{diag}\left(1, -(d-1), 1, \dots, 1\right), \quad (5)$$

where $f(\Omega)$ is the Casimir amplitude, Ω is the opening angle of wedge, and r is the distance to the corner of wedge. Similar to the strip, we propose the ratio of Casimir amplitude to the norm of displacement operator has a lower bound set by holography

$$\left(\frac{-f(\Omega)}{C_D}\right) \geq \lim_{T \rightarrow -(d-1)} \left(\frac{-f(\Omega)}{C_D}\right)_{\text{holo}}, \text{ for } 0 < \Omega \leq \pi. \quad (6)$$

In the following, we derive the holographic lower bound by Einstein's gravity and verify it by free BCFTs. See Fig. 7 and Fig. 8 for the ratios $(-f(\Omega)/C_D)$ for various 3d and 4d BCFTs. The holographic lower bound (6) is obtained analytically for $d = 2, 4$ and numerically for general dimensions. It suggests holography sets a lower bound of the Casimir effect for general boundary shapes, not limited to the strip.

The paper is organized as follows. In section 2, we study the holographic bound of the strip Casimir effect for DGP gravity in general dimensions. We show detailed calculations. We find two phases depending on the DGP couplings. The normal phase can continuously transform into that of Einstein's gravity and imposes a universal lower bound of the Casimir effect. The singular phase cannot continuously transform into that of Einstein's gravity and is always larger than the holographic lower bound. We generalize the discussions to GB gravity and GB-DGP gravity in section 3 and section 4, respectively. Section 5 tests the holographic lower bound of the strip Casimir effect. Section 6 discusses the holographic lower bound of the Casimir effect for a wedge. Finally, we conclude with some open problems in section 7. Appendix A and Appendix B derive the ghost-free condition and the norm of displacement operator for GB-DGP gravity.

2 Holography I: DGP gravity

In this section, we study the holographic bound of the Casimir effect of a strip for DGP gravity in general dimensions. Depending on the DGP parameters, there are two phases. The normal phase yields a universal lower bound of the Casimir effect. On the other hand, the singular phase obeys but cannot saturate the lower bound of the Casimir effect.

We start with the DGP gravity

$$I_{\text{DGP}} = \int_N d^{d+1}x \sqrt{|g|} \left(R + d(d-1) \right) + 2 \int_Q d^d y \sqrt{|h|} \left(K - T + \lambda \mathcal{R} \right), \quad (7)$$

where R is Ricci scalar in bulk N , K and \mathcal{R} are extrinsic curvature and Ricci scalar on the brane Q , T denotes the brane tension, and λ is the DGP coupling. For simplicity, we have set the Newton constant to be $16\pi G_N = 1$ and the AdS radius to be $l = 1$. We choose Neumann boundary condition (NBC) [23] on the brane Q

$$K^{ij} - (K - T + \lambda \mathcal{R})h^{ij} + 2\lambda \mathcal{R}^{ij} = 0, \quad (8)$$

where the brane tension is parameterized as [24]

$$T = (d-1) \tanh(\rho) - (d-1)(d-2)\lambda \operatorname{sech}^2(\rho). \quad (9)$$

Let us explain the origin of this parameterization. The local region near any smooth boundary can be approximately a half-space. Thus, the gravity dual of the near-boundary region is given by that of half space

$$\text{metric : } ds^2 = \frac{dz^2 - dt^2 + dx^2 + \sum_{a=1}^{d-2} dy_a^2 + O(z^2)}{z^2}, \quad (10)$$

$$\text{brane for half space } x \geq 0 : x = -\sinh(\rho)z + O(z^2), \quad (11)$$

$$\text{brane for half space } x \leq L : x - L = \sinh(\rho)z + O(z^2). \quad (12)$$

Then the NBC (8) at leading order yields (9). We focus on positive DGP gravity to be ghost-free [24]

$$\lambda \geq 0. \quad (13)$$

The holographic norm of displacement operator is given by [24, 25] for $\rho \leq 0$

$$C_D = \frac{2(d-1)\pi^{\frac{1}{2}-\frac{d}{2}}\Gamma(d+2)(-\operatorname{csch}(\rho))^{-d}}{\Gamma\left(\frac{d+1}{2}\right)\left(\frac{d\sinh(\rho)\cosh(\rho)(-\operatorname{coth}(\rho))^{3-d}}{2(d-2)\lambda+\operatorname{coth}(\rho)} - {}_2F_1\left(\frac{d-1}{2}, \frac{d}{2}; \frac{d+2}{2}; -\operatorname{csch}^2(\rho)\right)\right)}. \quad (14)$$

The one with $\rho \geq 0$ can be obtained by analytical continuation. For example, we have

$$C_D = \begin{cases} \frac{32}{\pi\left(\frac{2\lambda}{2\lambda\sinh(\rho)+\cosh(\rho)} + 2\tan^{-1}\left(\tanh\left(\frac{\rho}{2}\right) + \frac{\pi}{2}\right)\right)}, & \text{for } d = 3, \\ \frac{120e^{-\rho}(4\lambda\sinh(\rho)+\cosh(\rho))}{\pi^2(2\lambda\tanh(\rho)+2\lambda+1)}, & \text{for } d = 4. \end{cases} \quad (15)$$

$C_D \geq 0$ together with $\lambda \geq 0$ yields the constraints

$$0 \leq \lambda, \quad \text{for } \rho \geq 0, \quad (16)$$

$$0 \leq \lambda \leq -\frac{\operatorname{coth}(\rho)}{2(d-2)}, \quad \text{for } \rho \leq 0. \quad (17)$$

For $0 \leq \lambda \leq 1/2(d-2)$, the above constraints are automatically satisfied for arbitrary ρ . That is because $-\frac{\operatorname{coth}(\rho)}{2(d-2)} \geq \frac{1}{2(d-2)}$ for $\rho \leq 0$. While for $\lambda > 1/2(d-2)$, (17) sets a lower bound $\rho > -\operatorname{coth}^{-1}(2(d-2)\lambda)$. Thus, $\lambda = 1/2(d-2)$ is a critical DGP parameter. Below, we will show $\lambda = 1/2(d-2)$ is the phase-transition point for normal and singular phases.

2.1 General discussions

Now, let us study the gravity dual of a strip with width L . The vacuum of a trip is dual to the AdS soliton [26]

$$ds^2 = \frac{\frac{dz^2}{h(z)} + h(z)d\theta^2 - dt^2 + \sum_{a=1}^{d-2} dy_a^2}{z^2}, \quad (18)$$

where $h(z) = 1 - z^d/z_h^d$. To avoid conical singularities, we choose the angle period in bulk as

$$\beta = \frac{4\pi}{|h'(z_h)|} = \frac{4\pi z_h}{d}. \quad (19)$$

The strip is given by $0 \leq \theta \leq L$ on the AdS boundary $z = 0$. By applying the holographic renormalization [27], we derive the holographic energy density $T_{tt} = -1/z_h^d$. Compared with the Casimir effect (1), we get the holographic Casimir amplitude

$$\kappa_1 = \frac{L^d}{z_h^d}, \quad (20)$$

where the strip width L will be determined soon. Without loss of generality, we set $z_h = 1$ below. We label the embedding function of brane Q as

$$\theta = S(z). \quad (21)$$

Let us first study the case with negative brane tension $T \leq 0$, whose complement can give the other case with $T > 0$. It is the typical trick used in [26]. Let us explain more. See Fig. 1 for the geometry of the holographic dual of the strip. The region between red/blue curves (branes) and the black line is the bulk dual of strip I with $T \leq 0$; its complement in bulk is the gravity dual for strip II (green line) with $T > 0$. As shown in Fig. 1, the gravity duals of strip I and strip II share the same EOW branes (blue curve or red curve, depending on the theory parameters). As a result, the NBCs (8) for strips I and II take the same values. However, the extrinsic curvatures K_{ij} flip signs, while the induced metric h_{ij} and intrinsic Ricci tensor \mathcal{R}_{ij} remain invariant when crossing the branes. In the viewpoint of NBC (8), T and λ change signs equivalently when crossing the branes. Note that the bulk dual for strip II contains the ‘horizon’ $z = z_h$. To remove the conical singularity at $z = z_h$, we fix the period of angle θ as β (19). Thus, for $T > 0$, the left and right vertical dotted lines of Fig. 1 are identified due to the periodicity of angle θ . On the other hand, for the strip I with $T \leq 0$, the ‘horizon’ and potential conical singularity are hidden behind the branes (red/blue curves). Thus, the conical singularity is irrelevant, and θ can be non-periodic for $T \leq 0$ [29].

Below, we focus on the left half of branes with $T \leq 0$, the right half can be obtained by symmetry. Our convention of extrinsic curvature is $K = \nabla_\mu n^\mu$ with n the outward-pointing normal vector. On the left halves of the EOW branes, we have

$$n_\mu = \left(\frac{S'(z)}{\sqrt{\frac{z^2(h(z)^2 S'(z)^2 + 1)}{h(z)}}}, \frac{-1}{\sqrt{\frac{z^2(h(z)^2 S'(z)^2 + 1)}{f(z)}}}, 0, \dots, 0 \right). \quad (22)$$

Substituting (18), (21) and (22) into NBC (8), we get an independent equation for $T \leq 0$

$$T = -\frac{(d-1)h(z) \left((d-2)\lambda + h(z)S'(z)\sqrt{h(z)S'(z)^2 + \frac{1}{h(z)}} \right)}{h(z)^2 S'(z)^2 + 1}. \quad (23)$$

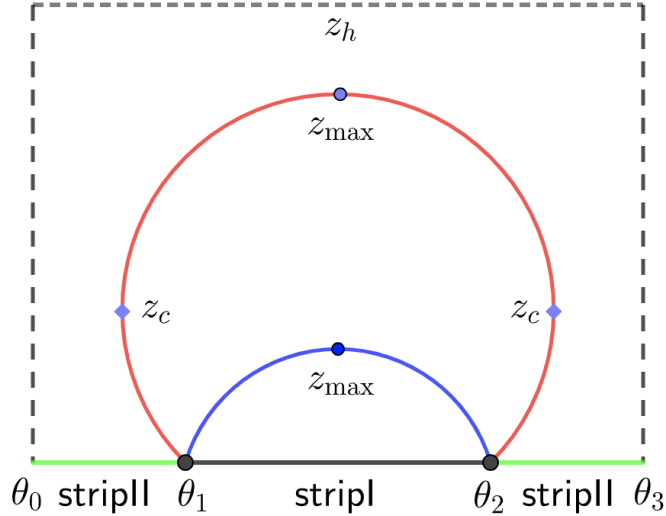


Figure 1: Geometry of holographic strip: a portion of AdS soliton. The region between red/blue curves (branes) and the black line is the bulk dual of strip I with negative brane tension $T \leq 0$; its complement in bulk is the gravity dual for strip II (green line) with $T > 0$. The gravity dual of strip II contains the ‘horizon’ $z = z_h$. The angle θ should be periodic to remove the conical singularity on it. Thus, the green lines for strip II are connected. Without loss of generality, we focus on strip I with $T \leq 0$. We have $(\rho < 0)$ and $(\rho > 0)$ for the blue and red curves, respectively. z_{\max} and z_c denote the turning points with $\theta'(z_{\max}) = \infty$ and $\theta'(z_c) = 0$.

Let us verify that it corresponds to the left half of branes. From (9,23), we derive $S'(0) = -\sinh(\rho)$ near θ_1 of Fig. 1, which agrees with (11) for the left boundary. As shown in Fig. 1, we have $S'(z_{\max}) = \infty$ and $S'(z_c) = 0$ at the turning points z_{\max} and z_c for the left halves of branes, respectively. Substituting $S'(z_{\max}) = \infty$ and $S'(z_c) = 0$ into (23), we obtain

$$T = -(d-1)\sqrt{h(z_{\max})} = -(d-1)(d-2)\lambda h(z_c). \quad (24)$$

Note that the turning point z_c appears only for the red curve of Fig. 1 with $\rho > 0$. Solving (23) and (24), we get

$$S'(z) = \pm \frac{\sqrt{2} \left(\sqrt{h(z_{\max})} - (d-2)\lambda h(z) \right)}{h(z) \sqrt{2(d-2)\lambda h(z) \sqrt{h(z_{\max})} + h(z)H(z) - 2h(z_{\max}) + h(z)}}, \quad (25)$$

where $H(z) = \sqrt{1 + 4(d-2)\lambda \left((d-2)\lambda h(z) - \sqrt{h(z_{\max})} \right)}$. We choose the positive sign, i.e., $S'(z) \sim \left(\sqrt{h(z_{\max})} - (d-2)\lambda h(z) \right)$, for the left halves of red and blue curves to get the correct behavior $S'(0) = -\sinh(\rho)$ near θ_1 of Fig. 1. The negative sign of (25) corresponds

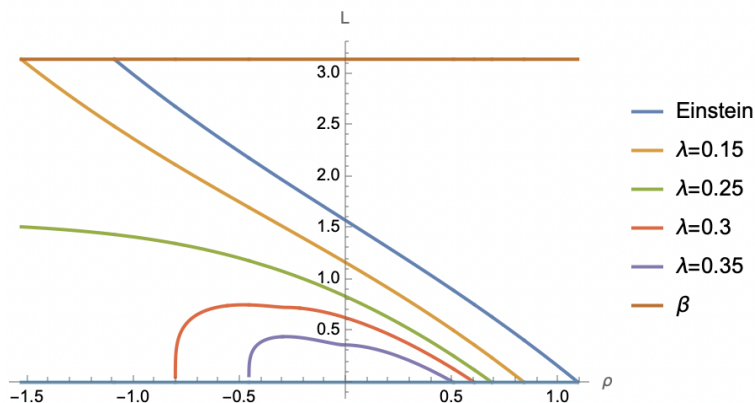


Figure 2: Strip widths in normal phase with $0 \leq \lambda < 1/4$ and singular phase $1/4 < \lambda \leq 1/2$ for $d = 4$. Note that L can be larger than β for negative enough ρ in the normal phase. We show only range of $L \leq \beta$ for simplicity. On the other hand, L is always smaller than β in the singular phase. In both cases, the condition $0 \leq L$ imposes an upper bound of ρ .

to the right halves of branes. From (21,25), we derive the width of strip I for $T \leq 0$

$$L_I = \int_0^{z_{\max}} dz \frac{2\sqrt{2} \left(\sqrt{h(z_{\max})} - (d-2)\lambda h(z) \right)}{h(z) \sqrt{2(d-2)\lambda h(z) \sqrt{h(z_{\max})} + h(z)H(z) - 2h(z_{\max}) + h(z)}}, \quad (26)$$

where $z_{\max} = (1 - T^2/(d-1)^2)^{1/d}$ from (24). We stress that the above formula works for both the cases of blue curve and red curve of Fig. 1. In particular, the integrand $2S'(z) \sim \left(\sqrt{h(z_{\max})} - (d-2)\lambda h(z) \right)$ flips signs at turning point z_c (24), which is the expected feature for the red curve. It suggests the integrand cannot be chosen as the absolute value $2|S'(z)| \sim \left| \sqrt{h(z_{\max})} - (d-2)\lambda h(z) \right|$, which misses the case of red curve. Recall that strip II is the complement of strip I and (T, λ) of NBC (8) flip signs when crossing the brane, we get the width of strip II for $T \geq 0$

$$L_{II} = \beta - L_I(T \rightarrow -T, \lambda \rightarrow -\lambda). \quad (27)$$

In total, we have

$$L = \begin{cases} L_I, & \text{for } T \leq 0, \\ L_{II}, & \text{for } T \geq 0. \end{cases} \quad (28)$$

One can check L is continuous at $T = 0$, which is a test of our results. See Fig. 2 for example.

Some comments are in order. First, (26) implies L_I could be negative ($L_{II} = \beta - L_I$ could be larger than β and result in conical singularity) for sufficiently large λ . To remove this unphysical case, we get an upper bound of the DGP coupling

$$\lambda \leq \frac{1}{d-2}. \quad (29)$$

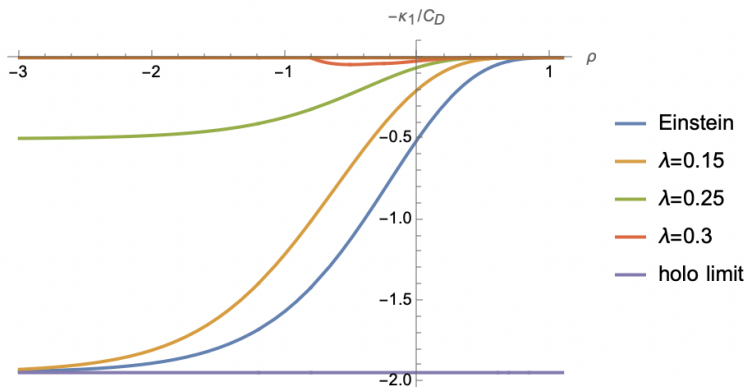


Figure 3: $(-\kappa_1/C_D)$ in normal phase $0 \leq \lambda \leq 1/4$ and singular phase with $1/4 < \lambda \leq 1/2$ for $d = 4$. In the normal phase, all curves approach the holographic limit (purple curve) from the above for $\rho \rightarrow -\infty$ ($T \rightarrow -3$). In the singular phase, $(-\kappa_1/C_D)$ is larger than the holographic limit (purple curve) and approach zero as $\lambda \rightarrow 1/2$.

It can be derived by considering the limit $z_{\max} \rightarrow 0$ ($T \rightarrow -(d-1)$). Then, $S'(z) \sim \left(\sqrt{h(z_{\max})} - (d-2)\lambda h(z) \right) \sim \left(1 - (d-2)\lambda \right) \geq 0$ yields (29). See also Fig. 2, which implies $L \rightarrow 0$ as $\lambda \rightarrow 1/(d-2)$. Second, the case $0 \leq \lambda < 1/2(d-2)$ can continuously transform into that of Einstein gravity, while the case $1/2(d-2) < \lambda \leq 1/(d-2)$ cannot. See Fig. 2 for instance. We name them normal and singular phases, respectively. Third, Fig. 2 shows the strip width L decreases with brane tension ρ in normal phase and $L \geq 0$ sets an upper bound of ρ [28] for fixed DGP parameter λ . For $T \geq 0$, L should be smaller than the angle period β to avoid the conical singularity. On the other hand, there is no upper bound of L for $T < 0$ since the conical singularity is hidden behind the brane [29]. Thus, it is irrelevant to the bulk dual of the strip. As a result, there is no extra constraint on the lower bound of T , and it can take the minimal value $T = -(d-1)$ ($\rho \rightarrow -\infty$) [28, 29].

We are prepared to analyze the $(-\kappa_1/C_D)$ ratio. The value of κ_1 can be determined from (20) with $z_h = 1$ and (26,27,28). The quantity C_D is given by (14,15). We present the graph of $(-\kappa_1/C_D)$ in Fig. 3. In the normal phase with $0 \leq \lambda < 1/2(d-2)$, the ratio $(-\kappa_1/C_D)$ increases with the tension ρ , reaching its minimum as $\rho \rightarrow -\infty$ ($T \rightarrow -(d-1)$). Notably, all curves converge to the same lower bound (purple curve) from above in the limit $\rho \rightarrow -\infty$ ($T \rightarrow -(d-1)$). We will provide an analytical proof of this observation in the following subsection. In the singular phase, $(-\kappa_1/C_D)$ is larger than the holographic limit (purple curve) and approaches zero as $\lambda \rightarrow 1/(d-2)$. Since we are interested in the lower bound of $(-\kappa_1/C_D)$, we focus on the normal phase below.

2.2 Analytical results

Let us have some analytical discussions. We are interested in the case with minimal tension $T \rightarrow -(d-1)$ in the normal phase since it gives the holographic lower bound of the Casimir effect. Performing coordinate transformation $z = z_{\max}y$ and expanding (26) around $x = \text{sech}^2(\rho) \rightarrow 0$ ($T \rightarrow -(d-1)$), we derive perturbatively in the normal phase

$$\begin{aligned} L_I &= \int_0^1 dy x^{1/d} \left(\frac{2(1-2(d-2)\lambda)^{\frac{1}{d}}}{\sqrt{1-y^d}\sqrt{x}} + O(\sqrt{x}) \right) \\ &= \frac{2x^{\frac{1}{d}-\frac{1}{2}}\sqrt{\pi}(1-2(d-2)\lambda)^{1/d}\Gamma(1+\frac{1}{d})}{\Gamma(\frac{1}{2}+\frac{1}{d})} + O(x^{\frac{1}{d}+\frac{1}{2}}). \end{aligned} \quad (30)$$

For $x \rightarrow 0$ ($T \rightarrow -(d-1)$), the displacement operator (14) becomes

$$C_D = \frac{2x^{1-\frac{d}{2}} \left((d-1)\pi^{\frac{1}{2}-\frac{d}{2}}(1-2(d-2)\lambda)\Gamma(d+2) \right)}{d\Gamma(\frac{d+1}{2})} + O(x^{2-\frac{d}{2}}). \quad (31)$$

In the limit $x \rightarrow 0$ ($T \rightarrow -(d-1)$), we obtain the universal lower bound (2) independent of λ

$$\lim_{T \rightarrow -(d-1)} \left(-\frac{\kappa_1}{C_D} \right) = \lim_{x \rightarrow 0} \left(-\frac{L_I^d}{C_D} \right) = -\frac{2^{d-2}d\pi^{d-\frac{1}{2}}\Gamma(\frac{d-1}{2})\Gamma(\frac{1}{d})^d}{\Gamma(d+2)(d\Gamma(\frac{1}{2}+\frac{1}{d}))^d}, \quad (32)$$

in the normal phase with $0 \leq \lambda < 1/2(d-2)$. Interestingly, unlike the KSS bound, holography imposes a universal lower bound of the Casimir effect. The following sections show this is also the case for GB gravity and GB-DGP gravity.

We need the negative brane tension to derive the holographic lower bound of the Casimir effect (32). Unlike the case of two-side branes in the discontinuous spacetime with non-trivial junction condition, the negative brane tension is well-defined on the one-side end-of-the-world (EOW) branes in AdS/BCFT [23, 26, 28, 29]. Recall that the brane tension flips signs when crossing the EOW brane in the continuous spacetime¹. If the positive brane tension is stable from the viewpoint of one side (gravity dual of strip II), so is the negative brane tension from the other side's perspective (gravity dual of strip I). Besides, the brane tension is a cosmological constant rather than a kinetic-energy term on the EOW brane. Of course, the negative cosmological constant is well-defined in AdS/CFT. One can prove the gravitational KK modes are ghost-free and tachyon-free on the EOW brane with general tensions (including negative brane tension) [24]. See Appendix A for an example. Finally, the negative brane tension would yield a negative A-type boundary central charge. But nothing goes wrong. Recall that the A-type boundary central charge is negative for a free scalar with the Dirichlet boundary condition [30]. For the reasons above, it is well-defined for the AdS/BCFT with a negative brane tension.

¹For the continuous spacetime, we have trivial junction condition $K_L{}_{ij} + K_R{}_{ij} = 0$ with $n_L = -n_R$ on the two sides of the brane.

3 Holography II: GB gravity

This section explores the holographic bound of the Casimir effect in Gauss-Bonnet (GB) gravity. Since the calculations are similar to those in DGP gravity, we will present only the key points below. We take the following form of GB action [31]²

$$I_{\text{GB}} = \int_N d^{d+1}x \sqrt{|g|} \left(R + d(d-1) + \alpha \mathcal{L}_{\text{GB}}(\bar{R}) \right) + 2 \int_Q d^d y \sqrt{|h|} \left((1 + 2(d-1)(d-2)\alpha)(K - T) + 2\alpha(J - 2G_Q^{ij}K_{ij}) \right), \quad (33)$$

where $\mathcal{L}_{\text{GB}}(\bar{R}) = \bar{R}_{\mu\nu\alpha\beta}\bar{R}^{\mu\nu\alpha\beta} - 4\bar{R}_{\mu\nu}\bar{R}^{\mu\nu} + \bar{R}^2$, \bar{R} is defined as

$$\bar{R} = R + d(d+1), \quad (34)$$

$$\bar{R}_{\mu\nu} = R_{\mu\nu} + dg_{\mu\nu}, \quad (35)$$

$$\bar{R}_{\mu\nu\rho\sigma} = R_{\mu\nu\rho\sigma} + (g_{\mu\rho}g_{\nu\sigma} - g_{\mu\sigma}g_{\nu\rho}), \quad (36)$$

which vanish on AdS space with unite radius. G_Q^{ij} is the intrinsic Einstein tensor on the boundary Q , and J is the trace of

$$J_{ij} = \frac{1}{3} \left(2KK_{ik}K_j^k - 2K_{ik}K^{kl}K_{lj} + K_{ij} \left(K_{kl}K^{kl} - K^2 \right) \right). \quad (37)$$

From action (33), we derive NBC on the brane Q

$$(1 + 2(d-1)(d-2)\alpha) \left(K^{ij} - (K - T)h^{ij} \right) + 2\alpha \left(H^{ij} - \frac{1}{3}Hh^{ij} \right) = 0, \quad (38)$$

where

$$H_{ij} = 3J_{ij} + 2K\mathcal{R}_{ij} + \mathcal{R}K_{ij} - 2K^{kl}\mathcal{R}_{kilj} - 4\mathcal{R}_{k(i}K_{j)}^k. \quad (39)$$

Following the same logic of sect. 2, we parameterize the brane tension as [31]

$$T = \frac{(d-1)\tanh(\rho)\text{sech}^2(\rho)((4\alpha(d-2)d+3)\cosh(2\rho) - 4\alpha(d-6)(d-2)+3)}{6 + 12\alpha(d-2)(d-1)}. \quad (40)$$

To avoid negative energy fluxes, the GB coupling α should obey [31, 32]

$$\frac{-1}{4(d^2 - 2d - 2)} \leq \alpha \leq \frac{1}{8}. \quad (41)$$

By applying the method of [24], we derive the ghost-free condition for gravitational KK modes of GB gravity (33)

$$\frac{\alpha \tanh(\rho)}{1 + 4\alpha(d-2)} \geq 0. \quad (42)$$

²Note that (33) is not the usual action of GB gravity. The relation to the usual one [32] can be found in [31]. We take the action (33) because it simplifies the calculations of displacement operator C_D . Besides, the AdS radius can be set to one $l = 1$ as Einstein gravity [31].

See appendix A for the derivation of (42) with $d = 4$. The norm of displacement operator is given by [31] for $\rho \leq 0$

$$C_D = -\frac{4\pi^{\frac{1}{2}-\frac{d}{2}}(4\alpha(d-2)+1)\Gamma(d+2)\cosh^d(\rho)\left((4\alpha(d-2)+1)\coth^2(\rho)+4\alpha(d-3)(d-2)\right)}{\Gamma\left(\frac{d-1}{2}\right)d(4\alpha(d-2)+1)\cosh^2(\rho)\coth^3(\rho)+G(-\coth(\rho))^d}, \quad (43)$$

where

$$G = \left((4\alpha(d-2)+1)\coth^2(\rho)+4\alpha(d-3)(d-2)\right) {}_2F_1\left(\frac{d-1}{2}, \frac{d}{2}; \frac{d+2}{2}; -\operatorname{csch}^2(\rho)\right). \quad (44)$$

Similar to DGP gravity, we can make analytical continuation to get C_D with $\rho \geq 0$. For $d = 4$, we get

$$(C_D)_{4d} = \frac{120(8\alpha+1)\coth(\rho)((16\alpha+1)\cosh(2\rho)+1)}{\pi^2(\coth(\rho)+1)(4\alpha\sinh(2\rho)+(12\alpha+1)\cosh(2\rho)+4\alpha+1)}. \quad (45)$$

The gravity dual of the vacuum of the strip is given by AdS soliton (18) with

$$h(z) = \frac{1+2\alpha(d-1)(d-2)-\sqrt{(1+4\alpha(d-2))^2+4\alpha(d-3)(d-2)(\alpha(d^2-d-2)+1)\frac{z^d}{z_h^d}}}{2\alpha(d-2)(d-3)}, \quad (46)$$

where $h(z_h) = 0$. Substituting the embedding function $\theta = S(z)$ and metric (18) into the NBC (38), we obtain one independent equation for the left halves of branes with $T \leq 0$

$$T = \frac{(1-d)h(z)S'(z)}{\sqrt{h(z)S'(z)^2+\frac{1}{h(z)}}} + \frac{2\alpha(d-1)(d-2)(d-3)h(z)^2S'(z)(h(z)^2S'(z)^2+3)}{3(1+2\alpha(d-1)(d-2))\sqrt{h(z)S'(z)^2+\frac{1}{h(z)}}(h(z)^2S'(z)^2+1)}. \quad (47)$$

Substituting the critical points $S'(z_{\max}) = \infty$ into the above equation, we get

$$T = \frac{(d-1)\sqrt{h(z_{\max})}(-6\alpha(d^2-3d+2)+2\alpha(d^2-5d+6)h(z_{\max})-3)}{6\alpha(d^2-3d+2)+3}. \quad (48)$$

From (47) and (48), we can solve $S'(z)$ in functions of $h(z)$ and $h(z_{\max})$. There are multiple solutions for $S'(z)$, and we choose the one that takes real values and can yield the correct limit $S'(0) = -\sinh(\rho)$ near θ_1 of Fig. 1. We do not show the complicated expression of $S'(z)$ for simplicity. From $S'(z)$, we can obtain the width for strip

$$L = \begin{cases} L_I = \int_0^{z_{\max}} 2S'(z)dz, & \text{for } T \leq 0, \\ L_{II} = \beta - L_I(\rho \rightarrow -\rho, \alpha \rightarrow \alpha), & \text{for } T \geq 0. \end{cases} \quad (49)$$

Note that the GB coupling α has different sign transformation rule from ρ in L_{II} . That is because α appears in terms like $K\mathcal{R}^2$ and K^3 on the brane, which flip signs when crossing the brane (similar to K). On the other hand, the tension T keeps invariant when crossing the brane. To keep the form of NBC (38) invariant, the tension T should flip signs while GB

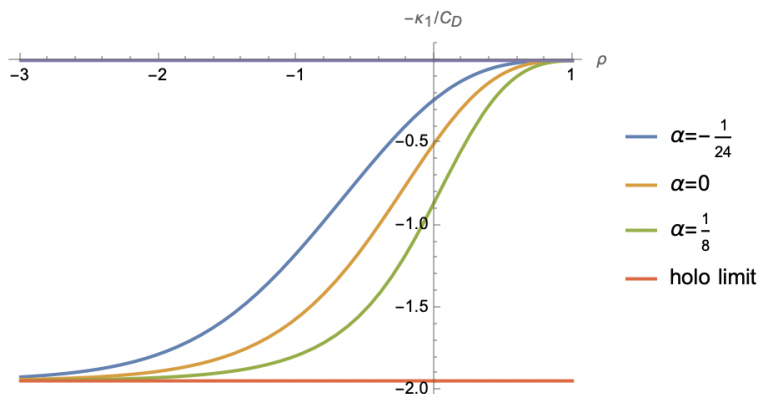


Figure 4: $(-\kappa_1/C_D)$ for GB gravity with $d = 4$. The blue, orange, green, red curves denote GB gravity with typical couplings $\alpha = (-\frac{1}{24}, 0, \frac{1}{8})$, and holographic limit (2), respectively. It shows GB gravity with various couplings α approach the same value in the limit $\rho \rightarrow -\infty$.

coupling α remains invariant when crossing the brane. By using the holographic renormalization for GB gravity [33], we obtain the energy density $T_{tt} = -(1 + \alpha(d-2)(d+1))/z_h^d$. Recall that $T_{tt} = -\kappa_1/L^d$ for a strip. Then, we get the holographic Casimir amplitude

$$\kappa_1 = \left(1 + \alpha(d-2)(d+1)\right) \frac{L^d}{z_h^d}. \quad (50)$$

Now we are ready to discuss the holographic lower bound of $(-\kappa_1/C_D)$. For simplicity, we set $z_h = 1$ below. We draw $(-\kappa_1/C_D)$ for GB gravity with typical couplings (41) for $d = 4$ in Fig. 4. Unlike DGP gravity, there is no singular phase for the GB gravity with couplings obeying (41). Like DGP gravity in the normal phase, $(-\kappa_1/C_D)$ for GB gravity increases with ρ and approaches the universal lower bound in the limit $\rho \rightarrow -\infty$. To end this section, we analytically derive the holographic lower bound of the Casimir effect for GB gravity. Fig. 4 shows the lower bound is saturated in the limit $x = \text{sech}^2(\rho) \rightarrow 0$ ($\rho \rightarrow -\infty$). In such limit, we can solve perturbatively $S'(z)$ from (47) and then derive the strip width (62)

$$\begin{aligned} L_I &= \int_0^1 dy \frac{2 \left(\frac{4\alpha(d-2)^2+1}{\alpha(d^2-d-2)+1} \right)^{1/d} x^{\frac{1}{d}-\frac{1}{2}}}{\sqrt{1-y^d}} + O(x^{\frac{1}{d}+\frac{1}{2}}) \\ &= \frac{2\sqrt{\pi} \left(\frac{4\alpha(d-2)^2+1}{\alpha(d^2-d-2)+1} \right)^{1/d} \Gamma(1+\frac{1}{d})}{\Gamma(\frac{1}{2}+\frac{1}{d})} x^{\frac{1}{d}-\frac{1}{2}} + O(x^{\frac{1}{d}+\frac{1}{2}}). \end{aligned} \quad (51)$$

For $x = \text{sech}^2(\rho) \rightarrow 0$, the displacement operator (43) becomes

$$C_D = \frac{x^{1-\frac{d}{2}} \left(2(d-1)\pi^{\frac{1}{2}-\frac{d}{2}} (4\alpha(d-2)^2+1) \Gamma(d+2) \right)}{d\Gamma(\frac{d+1}{2})} + O(x^{2-\frac{d}{2}}). \quad (52)$$

From (50,51,52) with $z_h = 1$, we finally derive the universal limit for GB gravity

$$\lim_{x \rightarrow 0} \left(-\frac{\kappa_1}{C_D} \right) = \lim_{x \rightarrow 0} \left(-\frac{\left(1 + \alpha(d-2)(d+1)\right) L_1^d}{C_D} \right) = -\frac{2^{d-2} d \pi^{d-\frac{1}{2}} \Gamma\left(\frac{d-1}{2}\right) \Gamma\left(\frac{1}{d}\right)^d}{\Gamma(d+2) \left(d \Gamma\left(\frac{1}{2} + \frac{1}{d}\right)\right)^d}, \quad (53)$$

which verifies again that holography imposes a universal lower bound (2) for the Casimir effect.

4 Holography III: GB-DGP gravity

This section studies the holographic bound of the Casimir effect in GB-DGP gravity. The qualitative behaviors of the Casimir effect in this context are similar to those observed in DGP and GB gravity. For simplicity, we focus on the dimension $d = 4$ and show only the key points below.

Let us quickly recall some key points. The action of GB-DGP gravity for $d = 4$ reads

$$I_{\text{GB-DGP}} = \int_N d^5 x \sqrt{|g|} \left(R + 12 + \alpha \mathcal{L}_{\text{GB}}(\bar{R}) \right) + 2 \int_Q d^4 y \sqrt{|h|} \left((1 + 12\alpha)(K - T + \lambda \mathcal{R}) + 2\alpha(J - 2G_Q^{ij} K_{ij}) \right), \quad (54)$$

with NBC on the brane

$$(1 + 12\alpha) \left(K^{ij} - (K - T + \lambda \mathcal{R}) h^{ij} + 2\lambda \mathcal{R}^{ij} \right) + 2\alpha \left(H^{ij} - \frac{1}{3} H h^{ij} \right) = 0, \quad (55)$$

where H is given by (39) and the brane tension is parameterized as

$$T = \frac{\text{sech}^3(\rho) (-24(12\alpha + 1)\lambda \cosh(\rho) + (32\alpha + 3) \sinh(3\rho) + 3 \sinh(\rho))}{48\alpha + 4}. \quad (56)$$

To avoid negative energy fluxes and to be ghost-free, the GB and DGP couplings should obey

$$\frac{-1}{24} \leq \alpha \leq \frac{1}{8}. \quad (57)$$

and

$$\frac{(1 + 12\alpha)\lambda + 2\alpha \tanh(\rho)}{1 + 8\alpha} \geq 0. \quad (58)$$

See Appendix A for the derivation of the ghost-free condition (58). The norm of displacement operator reads

$$C_D = \frac{240(8\alpha + 1)e^\rho \cosh(\rho) (4(12\alpha + 1)\lambda \sinh(2\rho) + (16\alpha + 1) \cosh(2\rho) + 1)}{\pi^2 (e^{4\rho} (16\alpha(3\lambda + 1) + 4\lambda + 1) + e^{2\rho} (8\alpha(6\lambda + 1) + 4\lambda + 2) + 8\alpha + 1)}, \quad (59)$$

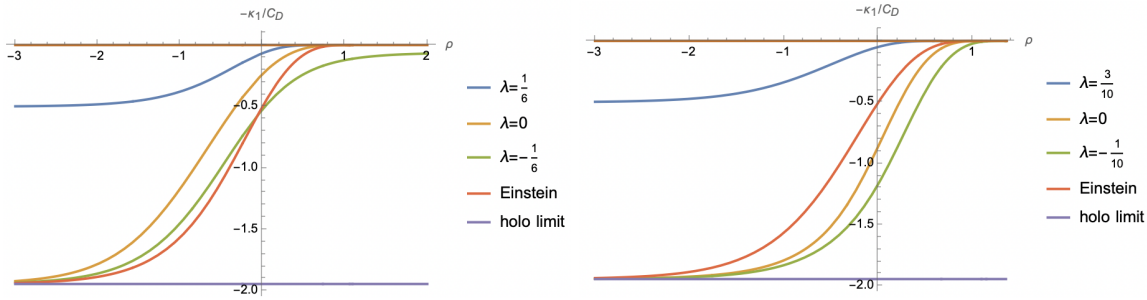


Figure 5: $(-\kappa_1/C_D)$ for GB-DGP gravity with $\alpha = -1/24$ (left) and $\alpha = 1/8$ (right). We focus on normal phase (63) and $d = 4$. The blue and green curves correspond to upper and lower bounds of (63). All curves except the blue ones approach the universal holographic limit (purple curve) for $\rho \rightarrow -\infty$. The blue curve corresponds to the critical point of normal and singular phases. For $\alpha = -1/24$ and $\lambda = -1/6$, $(-\kappa_1/C_D)$ (green curve) cannot approach zero.

where the calculations are given by Appendix B. Substituting the brane embedding function $\theta = S(z)$ and AdS soliton metric (18) into NBC (55), we get one independent equation for $T \leq 0$

$$T = -\frac{h(z) \left(6(12\alpha + 1)\lambda \sqrt{h(z)S'(z)^2 + \frac{1}{h(z)}} + h(z)^2(36\alpha - 4\alpha h(z) + 3)S'(z)^3 + (36\alpha - 12\alpha h(z) + 3)S'(z) \right)}{(12\alpha + 1)\sqrt{h(z)S'(z)^2 + \frac{1}{h(z)}}(h(z)^2S'(z)^2 + 1)}. \quad (60)$$

Substituting the critical points $S'(z_{\max}) = \infty$ and $S'(z_c) = 0$ into the above equation, we get

$$T = \sqrt{h(z_{\max})} \left(\frac{4\alpha h(z_{\max})}{12\alpha + 1} - 3 \right) = -6\lambda h(z_c). \quad (61)$$

From (60) and (61), we can express $S'(z)$ in terms of $f(z)$ and $f(z_{\max})$. There are multiple solutions for $S'(z)$, and we choose the real one with the correct limit $S'(0) = -\sinh(\rho)$ near θ_1 of Fig. 1. From $S'(z)$, we get the strip width

$$L = \begin{cases} L_I = \int_0^{z_{\max}} 2S'(z)dz, & \text{for } T \leq 0, \\ L_{II} = \beta - L_I(\rho \rightarrow -\rho, \lambda \rightarrow -\lambda, \alpha \rightarrow \alpha), & \text{for } T \geq 0. \end{cases} \quad (62)$$

Let us focus on the normal phase, which yields smaller $(-\kappa_1/C_D)$ than the singular phase. The parameter space for the normal phase is

$$-\frac{2\alpha \tanh(\rho)}{12\alpha + 1} \leq \lambda < \frac{1 + 16\alpha}{4(1 + 12\alpha)}, \quad (63)$$

where the lower bound is derived from the ghost-free condition (58) and the upper bound is obtained from $C_D \geq 0$ (59) or the small x expansion (64). Note that (63) reduces to the

normal phase $0 \leq \lambda < 1/4$ for DGP gravity with $\alpha = 0$, which is a test of our calculations. We draw $(-\kappa_1/C_D)$ for GB-DGP gravity in the normal phase in Fig. 5. It shows all curves except the blue ones approach the universal holographic limit (purple curve) for $\rho \rightarrow -\infty$. Note that the blue curve corresponds to the phase-transition point of normal and singular phases. It cannot saturate but still obeys the holographic lower bound (2). Following the method of sect.3.1, we consider the limit $x = \text{sech}^2(\rho) \rightarrow 0$ ($\rho \rightarrow -\infty$), which tends to give smaller $(-\kappa_1/C_D)$. In such limit, we can solve perturbatively $S'(z)$ from (60) and then derive the strip width (62) in the normal phase

$$L_I = 2\sqrt{\pi} \frac{\Gamma(\frac{5}{4})}{\Gamma(\frac{3}{4})} \left(\frac{1 - 4\lambda - 48\alpha\lambda + 16\alpha}{(1 + 10\alpha)x} \right)^{\frac{1}{4}} + O\left(x^{\frac{3}{4}}\right). \quad (64)$$

In the limit $x = \text{sech}^2(\rho) \rightarrow 0$, the norm of displacement operator (59) becomes

$$C_D = \frac{240(1 - 4\lambda - 48\alpha\lambda + 16\alpha)}{\pi^2 x} + O(x^0). \quad (65)$$

Then, we obtain the universal limit for the GB-DGP gravity in the normal phase

$$\lim_{x \rightarrow 0} \left(\frac{-\kappa_1}{C_D} \right) = \lim_{x \rightarrow 0} \frac{-(1 + 10\alpha)L_I^4}{C_D} = -\frac{\pi^4 \Gamma(\frac{5}{4})^4}{15\Gamma(\frac{3}{4})^4}, \quad (66)$$

which reproduces the lower bound (2) of Casimir effect for $d = 4$.

5 Tests of holographic bound

This section tests the Casimir effect's lower bound (2). We verify it by free scalars and fermions in general dimensions, Maxwell theory for $d = 4$ and $O(N)$ models in the $\epsilon = 4 - d$ expansions.

We first study free BCFTs. For free scalar with Robin boundary condition (RBC) and Dirichlet boundary condition (DBC), the Casimir amplitude [39] and displacement operator [25] are given by

$$(\kappa_1)_s = \frac{\zeta(d)\Gamma(\frac{d}{2})}{(4\pi)^{d/2}}, \quad (67)$$

$$(C_D)_s = \frac{\Gamma(\frac{d}{2})^2}{2\pi^d}, \quad (68)$$

which yields the ratio

$$\left(\frac{-\kappa_1}{C_D} \right)_s = -\frac{2^{1-d}\pi^{d/2}\zeta(d)}{\Gamma(\frac{d}{2})}. \quad (69)$$

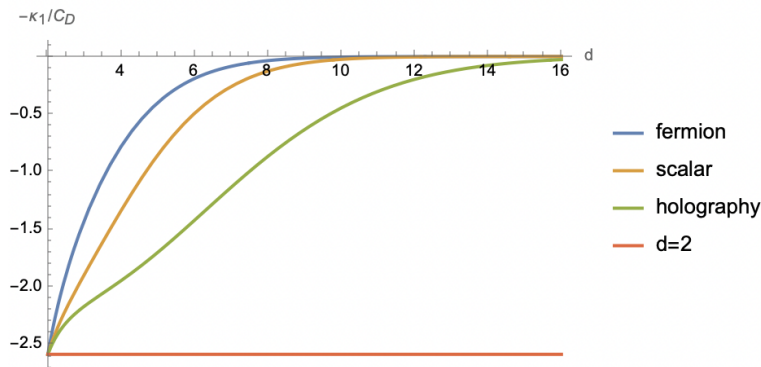


Figure 6: Various ratios $(-\kappa_1/C_D)$ in general dimensions. It shows $(-\kappa_1/C_D)_{\text{fermion}} \geq (-\kappa_1/C_D)_{\text{scalar}} \geq (-\kappa_1/C_D)_{\text{holo}}$. Besides, all ratios coincide for $d = 2$ and approach zero for $d \rightarrow \infty$.

For massless Dirac fermions, the Casimir amplitude [40] and displacement operator [42]³ read

$$(\kappa_1)_f = \frac{\zeta(d)\Gamma(\frac{d}{2})(1-2^{-(d-1)})2^{[\frac{d}{2}]}}{(4\pi)^{d/2}}, \quad (70)$$

$$(C_D)_f = (d-1)\pi^{-d}\Gamma\left(\frac{d}{2}\right)^2 2^{[\frac{d}{2}]-2}, \quad (71)$$

which gives

$$\left(\frac{-\kappa_1}{C_D}\right)_f = -\frac{4^{1-d}(2^d-2)\pi^{d/2}\zeta(d)}{(d-1)\Gamma(\frac{d}{2})}. \quad (72)$$

We draw various ratios $(-\kappa_1/C_D)$ in Fig. 6, which shows $(-\kappa_1/C_D)_f \geq (-\kappa_1/C_D)_s \geq (-\kappa_1/C_D)_{\text{holo}}$ in general dimensions. For $d = 2$, all ratios coincide

$$\left(\frac{-\kappa_1}{C_D}\right)|_{d=2} = -\frac{\pi^3}{12} \approx -2.58, \quad (73)$$

which is the expected result for 2d BCFTs⁴. Besides, all ratios approach zero as $d \rightarrow \infty$.

Let us go on to discuss Maxwell's theory for $d = 4$. We have

$$(\kappa_1)_M = \frac{\pi^2}{720}, \quad (C_D)_M = \frac{6}{\pi^4}, \quad (74)$$

³In the notation of [42], we have $C_D = \alpha(1) = -(d-1)\beta(1)$. Note that we have replaced $2^{\frac{d}{2}}$ of [42] with $2^{[\frac{d}{2}]}$, since we adopt $N \times N$ gamma matrices with $N = 2^{[\frac{d}{2}]}$.

⁴For $d = 2$, the strip Casimir effect can be obtained from that of half space by the conformal map. As a result, we have $\kappa_1 = c\pi/24$ [43] and $C_D = c/(2\pi^2)$. Thus, we have universally $(-\kappa_1/C_D) = -\pi^3/12$ for 2d BCFTs. Note that we impose the same conformal boundary conditions on the two boundaries of the strip.

which yields

$$\left(\frac{-\kappa_1}{C_D}\right)|_M = -\frac{\pi^6}{4320} \approx -0.22. \quad (75)$$

We summarize various free BCFTs for $d = 3$ and $d = 4$ in Table. 1, which all obeys the holographic lower bound (2) of Casimir effect.

We focus on the free BCFTs above. Now, let us consider BCFTs with interactions. We remark that the 3d Ising model and $O(N)$ model with $N = 2, 3$ obey the lower bound (2) of the Casimir effect [14]. Consider $O(N)$ in the $\epsilon = 4 - d$ expansions. The Casimir amplitude [41] and the norm of Casimir displacement operator [42] are given by

$$(\kappa_1)_{O(N)} = \frac{\pi^2 N}{1440} \left(1 + \epsilon \left(\frac{\gamma - 1}{2} - \frac{5(N+2)}{4(N+8)} - \frac{\zeta'(4)}{\zeta(4)} + \log(2\sqrt{\pi}) \right) \right), \quad (76)$$

$$(C_D)_{O(N)} = \frac{N}{2\pi^4} \left(1 + \epsilon \left(\gamma \pm \frac{5(N+2)}{6(N+8)} + \log(\pi) - 1 \right) \right), \quad (77)$$

where \pm denotes RBC and DBC. We get the ratio

$$\left(\frac{-\kappa_1}{C_D}\right)|_{O(N)} = \frac{-\pi^6}{720} \left(1 + \epsilon \left(\frac{1 - \gamma}{2} - \frac{90\zeta'(4)}{\pi^4} \mp \frac{5(N+2)}{6(N+8)} - \frac{5(N+2)}{4(N+8)} + \log\left(\frac{2}{\sqrt{\pi}}\right) \right) \right), \quad (78)$$

where $\gamma \approx 0.58$ is Euler's constant. Note that the ratio (78) is larger than that of free scalar (69) with $d = 4 - \epsilon$

$$\left(\frac{-\kappa_1}{C_D}\right)|_{O(N)} - \left(\frac{-\kappa_1}{C_D}\right)|_s \approx \frac{\pi^6(N+2)}{1728(N+8)}(3 \pm 2)\epsilon > 0. \quad (79)$$

Thus, it obeys the holographic lower bound (2). Here we require $\epsilon = g(N+8)/48\pi^2 > 0$ to avoid negative ϕ^4 interaction. Usually, a bound is set either by free theories or strongly coupled CFTs dual to gravity. For example, the Bueno-Casini-Andino-Moreno bound for entanglement entropy is set by free scalar [34], while the KSS bound for the fluid is set by holography [13]. The $O(N)$ in the $\epsilon = 4 - d$ expansion suggests that the free scalar may set the lower bound of the Casimir effect. However, the $O(N)$ models in non-integer dimensions are non-unitary [35]. On the other hand, the Ising with $d = 3$ confirms that holography, instead of the free scalar, sets the lower bound of the Casimir effect [14, 36, 37, 38].

6 Holographic bound for wedge

This section investigates the holographic bound of the Casimir effect for a wedge, which is the simplest generalization of a strip. For simplicity, we focus on Einstein's gravity and leave the discussions of higher derivative gravity to future work. Recall the wedge Casimir effect

takes the form (5) in a ground state. The wedge Casimir amplitude $f(\Omega)$ has two interesting limits

$$f(\Omega) \rightarrow \begin{cases} \kappa_1/\Omega^d, & \text{for } \Omega \rightarrow 0, \\ \kappa_2(\pi - \Omega), & \text{for } \Omega \rightarrow \pi, \end{cases} \quad (80)$$

where κ_1 is the strip Casimir amplitude (1), and κ_2 is universally determined by the displacement operator [21]

$$\kappa_2 = \frac{d\pi^{\frac{d-2}{2}}\Gamma(\frac{d}{2})}{2(d-1)\Gamma[d+2]}C_D. \quad (81)$$

The bound of κ_1 (2) and the universal relation (81) suggest the following lower bound for wedge space

$$\left(\frac{-f(\Omega)}{C_D}\right) \geq \lim_{T \rightarrow -(d-1)} \left(\frac{-f(\Omega)}{C_D}\right)_{\text{holo}}, \text{ for } 0 < \Omega \leq \pi. \quad (82)$$

In the following, we derive the holographic lower bound above and verify it by free BCFTs.

The gravity dual of wedge space is given by AdS soliton with the metric [21]

$$ds^2 = \frac{\frac{dz^2}{h(z)} + h(z)d\theta^2 + \frac{dr^2 + \sum_{i,j=1}^{d-2} \eta_{ij} dy^i dy^j}{r^2}}{z^2}, \quad (83)$$

where $h(z) = 1 - z^2 - c_1 z^d$. It produces the expected Casimir effect (5) provided [21]

$$c_1 = f(\Omega) = z_{\text{max}}^{-d} (\text{sech}^2(\rho) - z_{\text{max}}^2), \quad (84)$$

where z_{max} is the turning point. From NBC (8) with $\lambda = 0$, we can fix the opening angle of the wedge as [21]

$$\Omega_{\text{I}} = 2 \int_0^{z_{\text{max}}} \frac{dz}{h(z) \sqrt{\frac{h(z)}{h(z_{\text{max}})} - 1}}, \text{ for } T \leq 0, \quad (85)$$

and

$$\Omega_{\text{II}} = \beta - \Omega_{\text{I}}(\rho \rightarrow -\rho), \text{ for } T \geq 0. \quad (86)$$

Here β is the angle period in bulk

$$\beta = \frac{4\pi}{|h'(z_h)|} = \frac{4\pi z_h}{d + (2-d)z_h^2}, \quad (87)$$

with $h(z_h) = 0$. From (84,85,86), we can derive $f(\Omega)$ for any given brane tension $T = (d-1)\tanh(\rho)$. $f(\Omega)$ is obtained exactly for $d = 2, 4$ and numerically for general d [21]. The norm of the displacement operator reads [21]

$$C_D = \frac{2(d-1)\Gamma(d+2)}{d\pi^{\frac{d-2}{2}}\Gamma(\frac{d}{2})} \begin{cases} \frac{-d\Gamma(\frac{d}{2})\text{sech}^3(\rho)(-\text{csch}(\rho))^{-d}}{\sqrt{\pi}\Gamma(\frac{d+1}{2})(\text{sech}^3(\rho)^F + d\text{csch}(\rho)(-\tanh(\rho))^d)}, & \text{for } \rho \leq 0, \\ \frac{d\Gamma(\frac{d}{2})}{\pi(d-1)d\Gamma(\frac{d}{2}) - \frac{\sqrt{\pi}\Gamma(\frac{d+1}{2})(d(\tanh(\rho)\text{sech}(\rho))^d - \sinh(\rho)\text{sech}^{d+3}(\rho)F)}}{\text{sech}^2(\rho)\tanh^{d+1}(\rho)}, & \text{for } \rho \geq 0, \end{cases} \quad (88)$$

where $F = {}_2F_1\left(\frac{d-1}{2}, \frac{d}{2}; \frac{d+2}{2}; -\text{csch}^2(\rho)\right)$. In the limit $x = \text{sech}^2(\rho) \rightarrow 0$, we have

$$C_D = \frac{2(d-1)\pi^{\frac{1}{2}-\frac{d}{2}}\Gamma(d+2)}{d\Gamma\left(\frac{d+1}{2}\right)}x^{1-\frac{d}{2}} + O\left(x^{2-\frac{d}{2}}\right). \quad (89)$$

Now let us consider the holographic lower bound (82). Similar to the case of the strip, the lower bound (82) is achieved with the minimal brane tension $T \rightarrow -(d-1)$ ($\rho \rightarrow -\infty$). To have a finite ratio $-f(\Omega)/C_D$, we consider the limit $x \rightarrow 0$, $f(\Omega) \rightarrow \infty$ with $\hat{f}(\Omega) = f(\Omega)x^{\frac{d}{2}-1}$ finite. Then, the ratio becomes

$$\text{ra}(\Omega) = \lim_{x \rightarrow 0} \left(\frac{-f(\Omega)}{C_D} \right) = \lim_{x \rightarrow 0} \frac{-f(\Omega)x^{\frac{d}{2}-1}}{\frac{2(d-1)\pi^{\frac{1}{2}-\frac{d}{2}}\Gamma(d+2)}{d\Gamma\left(\frac{d+1}{2}\right)}} = \frac{-\hat{f}(\Omega)}{\frac{2(d-1)\pi^{\frac{1}{2}-\frac{d}{2}}\Gamma(d+2)}{d\Gamma\left(\frac{d+1}{2}\right)}} \quad (90)$$

From (84), we solve

$$z_{\max} = z_0\sqrt{x}, \quad \text{with } \hat{f}z_0^d + z_0^2 - 1 = 0. \quad (91)$$

Substituting (91) together with $c_1 = f = \hat{f}x^{1-\frac{d}{2}}$ into (85) and taking the limit $x \rightarrow 0$, we obtain

$$\Omega = \int_0^1 dy \frac{2z_0}{\sqrt{1-y^2z_0^2 + (z_0^2-1)y^d}}, \quad (92)$$

where z_0 is a function of \hat{f} from (91). We remark that (92) gives the correct limit (80) for $f = \hat{f} = 0$ ($z_0 = 1$)

$$\lim_{f \rightarrow 0} \Omega = \int_0^1 dy \frac{2}{\sqrt{1-y^2}} = \pi, \quad (93)$$

which is a test of our calculations. For $d = 2, 4$, we derive exact expressions

$$\Omega = \begin{cases} \pi z_0, & \text{for } d = 2, \\ 2z_0 K(z_0^2 - 1), & \text{for } d = 4, \end{cases} \quad (94)$$

where K denotes the complete elliptic integral of the first kind. From (90) and (91), we can express z_0 in terms of the ratio ra (90) and then rewrite (94) as

$$\Omega = \begin{cases} \frac{\pi^{3/2}}{\sqrt{\pi-12\text{ra}}}, & \text{for } d = 2, \\ \frac{1}{2} \sqrt{\frac{\pi}{30}} \sqrt{\frac{\pi-\sqrt{\pi^2-960\text{ra}}}{\text{ra}}} K\left(\frac{\pi(\pi-\sqrt{\pi^2-960\text{ra}})}{480\text{ra}} - 1\right), & \text{for } d = 4. \end{cases} \quad (95)$$

Now we have obtained the exact relations between the ratio $\text{ra} = (-f(\Omega)/C_D)$ and the opening angle Ω in the limit $T \rightarrow -(d-1)$ for $d = 2, 4$. For general dimensions, we can

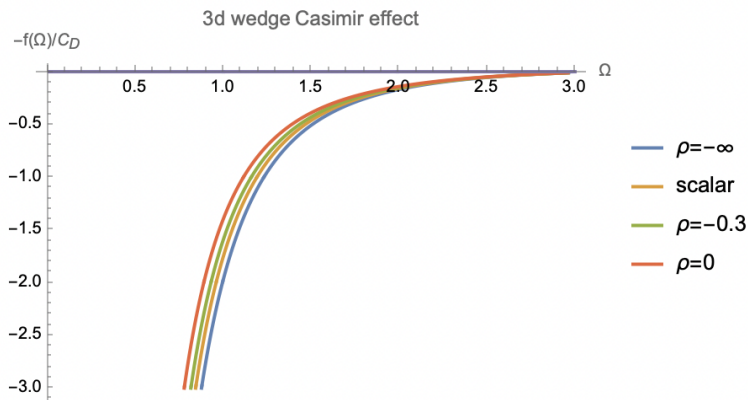


Figure 7: $(-f(\Omega)/C_D)$ for 3d BCFTs. The blue, green, red and yellow curves correspond to AdS/BCFT with $\rho = -\infty, -0.3, 0$, and free scalar. It shows holography with $T \rightarrow -2$ ($\rho \rightarrow -\infty$) (blue curve) sets the lower bound of wedge Casimir effect.

derive $\text{ra}(\Omega)$ numerically from (90,91,92). To end this section, we draw $(-f(\Omega)/C_D)$ for free and holographic BCFTs in Fig. 7 for $d = 3$ and Fig. 8 for $d = 4$. The expressions of $f(\Omega)$ for free BCFTs can be found in [21]. Fig. 7 and Fig. 8 show the AdS/BCFT with the minimal tension $T \rightarrow -(d-1)$ imposes the lower bound of wedge Casimir effect. The results of this section imply that holography sets a lower bound of the Casimir effect for general boundary shapes, not just for the strip. We leave the study of general boundary shapes to future work. We remark that the holographic lower bound for the wedge Casimir effect is independent of the gravity models. We have checked that DGP gravity in the normal phase yields the same results as Einstein gravity.

7 Conclusions and Discussions

In this paper, we explore the fundamental bound of the Casimir effect in general dimensions. We propose holography impose a universal lower bound on the Casimir coefficient ratio to the displacement operator norm. It is similar to the famous KSS bound [13] for hydromechanics and sheds light on the crucial question: how large the Casimir effect one could produce in principle. We derive the universal bound for a strip by studying various holographic models and verify it with free BCFTs and the $O(N)$ model in ϵ expansions. We also derive the holographic bound of the Casimir effect for a wedge and test it with free BCFTs. Our proposal is expected to work for general boundary shapes, not limited to the strip and wedge.

There are many essential problems worth exploring.

- It is interesting to find a field-theoretical proof or counterexample of the holographic

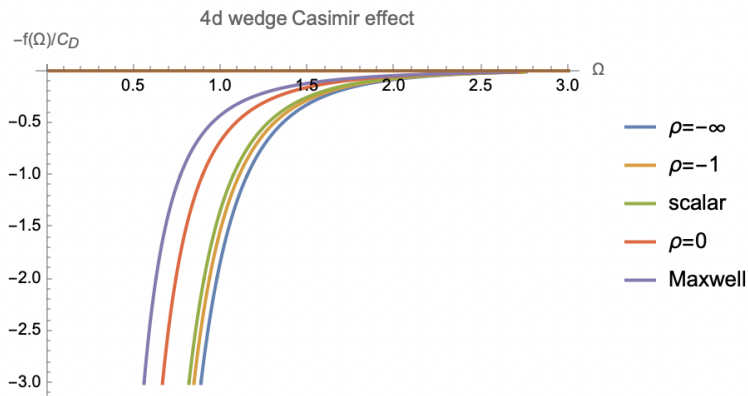


Figure 8: $(-f(\Omega)/C_D)$ for 4d BCFTs. The blue, yellow, red, green, and purple curves correspond to AdS/BCFT with $\rho = -\infty, -1, 0$, scalar and Maxwell field. It shows holography with $T \rightarrow -3$ ($\rho \rightarrow -\infty$) (blue curve) sets the lower bound of wedge Casimir effect.

bounds (2,6). The conformal bootstrap is a powerful tool for achieving this target.

- This paper focuses on the Casimir effect of the strip and wedge. It is interesting to generalize the discussions to general boundary shapes. Near a curved boundary, the Casimir effect takes a universal form determined by Weyl anomaly [44]

$$\langle T_{ij} \rangle = \alpha_1 \frac{\bar{k}_{ij}}{x^{d-1}} + \dots, \quad r \sim 0, \quad (96)$$

where \bar{k}_{ij} are the traceless parts of extrinsic curvatures, x is the distance to the boundary, and α_1 is boundary central charge of Weyl anomaly, or equivalently, the norm of displacement operator [25]

$$\alpha_1 = -\frac{d\Gamma[\frac{d+1}{2}]\pi^{\frac{d-1}{2}}}{(d-1)\Gamma[d+2]}C_D. \quad (97)$$

We get finite terms by subtracting the divergent terms (96) from the Casimir effect. The ratios of these finite terms and C_D are expected to have a universal lower bound. We leave this non-trivial problem to future work.

- For simplicity, this paper focuses on BCFTs. It is interesting to generalize our proposal to non-BCFTs. Let us consider the massive free theories. For non-BCFTs, we define the norm of displacement operator in the short-distance limit

$$\langle D(y)D(0) \rangle = \frac{C_D}{|y|^{2d}} + O(|y|^{2d-1}). \quad (98)$$

By dimensional analysis, C_D is independent of the mass. It agrees that the mass effect can be ignored at UV, i.e., $my \ll 1$. On the other hand, the Casimir effect is suppressed by the mass [8]. As a result, the ratios, such as $(-\kappa_1/C_D)$ and $(-f(\Omega)/C_D)$, increase with the mass and thus obey the lower bounds (2,6) of Casimir effect. Exploring the scope within which the holographic bound is obeyed for non-BCFT is interesting.

- For simplicity, we impose the same boundary conditions on the two boundaries of the strip and wedge. It is interesting to generalize to the case of mixed boundary conditions. The gravity dual of mixed boundary conditions can be realized by adding matter fields on the branes. The corresponding study is ongoing.

Acknowledgements

We thank T. Takayanagi, J. X. Lu, S. Lin, W. L. Li, Z. J. Li, N. Su for valuable comments and discussions. We are grateful to W. z. Guo, L. Y. Huang, S. He, S. M. Ruan and many participants of ‘‘Gauge Gravity Duality 2024’’ for helpful discussions. This work is supported by the National Natural Science Foundation of China (No.12275366).

A Ghost-free condition for GB-DGP gravity

Following the approach of [24], we derive the ghost-free condition (42) for GB-DGP gravity (33) with $d = 4$ in this appendix. We take the following ansatz of the perturbation metric and the embedding function of the brane

$$ds^2 = dr^2 + \cosh^2(r) \left(\bar{h}_{ij}^{(0)}(y) + \epsilon H(r) \bar{h}_{ij}^{(1)}(y) \right) dy^i dy^j + O(\epsilon^2), \quad (99)$$

$$Q : r = \rho + O(\epsilon^2), \quad (100)$$

where $\bar{h}_{ij}^{(0)}$ is the AdS metric with a unit radius and $\bar{h}_{ij}^{(1)}$ denotes the perturbation. Under the transverse traceless gauge

$$\bar{D}^i \bar{h}_{ij}^{(1)} = 0, \quad \bar{h}^{(0)ij} \bar{h}_{ij}^{(1)} = 0, \quad (101)$$

the equations of motion (EOM) of GB-DGP gravity can be separated variables as

$$(\bar{\square} + 2 - m^2) \bar{h}_{ij}^{(1)}(y) = 0, \quad (102)$$

$$\cosh^2(r) H''(r) + 4 \sinh(r) \cosh(r) H'(r) + m^2 H(r) = 0, \quad (103)$$

where m is the graviton mass. We impose DBC on the AdS boundary while NBC (38) on the brane, which yields

$$H(-\infty) = 0, \quad (104)$$

$$H'(\rho) = 2m^2 H(\rho) \operatorname{sech}^2(\rho) \left(\frac{\lambda + 12\alpha\lambda + 2\alpha \tanh(\rho)}{1 + 8\alpha} \right). \quad (105)$$

From EOM (103) and BCs (104,105), we derive the orthogonal relationship for KK modes

$$\langle H_m, H_{m'} \rangle = c_m \delta_{m,m'} = \int_{-\infty}^{\rho} \frac{\cosh^2(r)}{\cosh^2(\rho)} H_m(r) H_{m'}(r) dr$$

$$+ 2\left(\frac{\lambda + 12\alpha\lambda + 2\alpha \tanh(\rho)}{1 + 8\alpha}\right)H_m(\rho)H_{m'}(\rho). \quad (106)$$

To have a positive inner product $c_m = \langle H_m, H_m \rangle$, both the bulk integral and boundary term of (106) should be positive, which gives the ghost-free condition (42). Let us provide solid proof of this statement below.

Defining the step function

$$\Pi_0(r) = \begin{cases} 0, & \text{for } r < \rho, \\ 1, & \text{for } r \geq \rho. \end{cases} \quad (107)$$

and expanding it in terms of KK modes, we obtain

$$\Pi_0(r) = \sum_m \frac{\langle \Pi_0, H_m \rangle}{\langle H_m, H_m \rangle} H_m(r) = 2\left(\frac{\lambda + 12\alpha\lambda + 2\alpha \tanh(\rho)}{1 + 8\alpha}\right) \sum_m \frac{H_m(\rho)H_m(r)}{\langle H_m, H_m \rangle}, \quad (108)$$

where we have used $\langle \Pi_0, H_m \rangle = 2\left(\frac{\lambda + 12\alpha\lambda + 2\alpha \tanh(\rho)}{1 + 8\alpha}\right)H_m(\rho)$ derived from (106,108). Noting that $\Pi_0(\rho) = 1$, the above equation yields the so-called spectrum identity

$$\sum_m \frac{H_m(\rho)H_m(\rho)}{\langle H_m, H_m \rangle} = \frac{1}{2\left(\frac{\lambda + 12\alpha\lambda + 2\alpha \tanh(\rho)}{1 + 8\alpha}\right)}. \quad (109)$$

For a ghost-free theory with $\langle H_m, H_m \rangle > 0$, the left-hand side of (109) is positive. As a result, the right-hand side of (109) must also be positive, which gives the ghost-free condition (42)

$$\frac{\lambda + 12\alpha\lambda + 2\alpha \tanh(\rho)}{1 + 8\alpha} \geq 0. \quad (110)$$

According to [24], the KK modes are automatically tachyon-free under the ghost-free condition (110). First, let us prove the mass spectrum is real. If there were complex m^2 , they must appear in a complex conjugate pair, since both the EOM (105) and BCs (104,105) are real. Then the orthogonal condition (106) becomes

$$\langle H_m, H_{m^*} \rangle = \int_{-\infty}^{\rho} \frac{\cosh^2(r)}{\cosh^2(\rho)} |H_m(r)|^2 dr + 2\left(\frac{\lambda + 12\alpha\lambda + 2\alpha \tanh(\rho)}{1 + 8\alpha}\right) |H_m(\rho)|^2 > 0. \quad (111)$$

On the other hand, we have $\langle H_m, H_{m^*} \rangle = c_m \delta_{m,m^*} = 0$. The contradiction means there are no complex masses for the KK modes. Let us go on to prove $m^2 > 0$. From EOM (105) and BCs (104,105), we derive

$$\begin{aligned} & \int_{-\infty}^{\rho} \cosh^4(r) H_m'(r) H_m'(r) dr = \cosh^4(\rho) H_m'(\rho) H_m(\rho) - \int_{-\infty}^{\rho} (\cosh^4(r) H_m'(r))' H_m(r) dr \\ & = m^2 \left[\int_{-\infty}^{\rho} \cosh^2(r) H_m^2(r) dr + 2\left(\frac{\lambda + 12\alpha\lambda + 2\alpha \tanh(\rho)}{1 + 8\alpha}\right) \cosh^2(\rho) H_m^2(\rho) \right] \end{aligned}$$

$$= m^2 \langle H_m, H_m \rangle \cosh^{d-2}(\rho). \quad (112)$$

Because $\int_{-\infty}^{\rho} \cosh^4(r) H'_m(r) H'_m(r) dr$ and $\langle H_m, H_m \rangle$ are both positive, the above equation leads to $m^2 > 0$.

We have obtained the ghost-free condition (110) and prove it automatically yields a tachyon-free mass spectrum. Note that the brane tension can be negative in the above discussions. For example, ρ can be negative in the orthogonal condition (106) and all the conclusions derived from it. A quick way to see this is by considering Einstein's gravity with $\lambda = \alpha = 0$. Thus, we confirm that the negative brane tension is well-defined in AdS/BCFT, as we stressed in the main text.

B Displacement operator for GB-DGP gravity

By applying the method of [44], we derive the norm of displacement operator for GB-DGP gravity (42) with $d = 4$ in this appendix. We consider the perturbative metric of a half-space

$$ds^2 = \frac{1}{z^2} \left[dz^2 + dx^2 + \left(\delta_{ab} - 2\epsilon x \bar{k}_{ab} f\left(\frac{z}{x}\right) \right) dy^a dy^b + O(\epsilon^2) \right], \quad (113)$$

and the embedding function of brane Q

$$x = -\sinh \rho z + O(\epsilon^2), \quad (114)$$

where ϵ denotes the expanding order. We impose DBC $f(0) = 1$ on the AdS boundary $z = 0$ so that \bar{k}_{ab} become the traceless parts of extrinsic curvatures for BCFTs. Substituting (113) into EOM of GB-DGP gravity, we get one independent equation

$$s(s^2 + 1) f''(s) - 3f'(s) = 0, \quad (115)$$

which can be solved as

$$f(s) = 1 + 2d_1 - d_1 \frac{(2 + s^2)}{\sqrt{1 + s^2}}. \quad (116)$$

Above, we have used $f(0) = 1$ to fix one integral constant. Substituting (116) and (113,114) into NBC (38), we determine the other integral constant

$$d_1 = -\frac{e^\rho \cosh(\rho)(4(12\alpha + 1)\lambda \sinh(2\rho) + (16\alpha + 1) \cosh(2\rho) + 1)}{e^{4\rho}(16\alpha(3\lambda + 1) + 4\lambda + 1) + e^{2\rho}(8\alpha(6\lambda + 1) + 4\lambda + 2) + 8\alpha + 1}. \quad (117)$$

From (113,116), we derive the holographic stress tensor for GB gravity [33]

$$\langle T_{ab} \rangle = 2(1 + 8\alpha) d_1 \frac{\epsilon \bar{k}_{ab}}{x^3} + O(\epsilon^2). \quad (118)$$

Comparing (118) with (96), we read off $2(1 + 8\alpha) d_1 = \alpha_1$. Then from (97) and (117), we finally obtain the norm of displacement operator (45) for GB-DGP gravity

$$C_D = \frac{240(8\alpha + 1)e^\rho \cosh(\rho)(4(12\alpha + 1)\lambda \sinh(2\rho) + (16\alpha + 1) \cosh(2\rho) + 1)}{\pi^2 (e^{4\rho}(16\alpha(3\lambda + 1) + 4\lambda + 1) + e^{2\rho}(8\alpha(6\lambda + 1) + 4\lambda + 2) + 8\alpha + 1)}. \quad (119)$$

References

- [1] U. Mohideen and A. Roy, Phys. Rev. Lett. **81**, 4549-4552 (1998)
- [2] G. Bressi, G. Carugno, R. Onofrio and G. Ruoso, Phys. Rev. Lett. **88**, 041804 (2002)
- [3] G. L. Klimchitskaya, U. Mohideen and V. M. Mostepanenko, Rev. Mod. Phys. **81**, 1827-1885 (2009)
- [4] H. B. G. Casimir, Indag. Math. **10**, no.4, 261-263 (1948)
- [5] G. Plunien, B. Muller and W. Greiner, Phys. Rept. **134**, 87-193 (1986)
- [6] M. Bordag, U. Mohideen and V. M. Mostepanenko, Phys. Rept. **353**, 1-205 (2001)
- [7] K. A. Milton, J. Phys. A **37**, R209 (2004)
- [8] M. Bordag, G. L. Klimchitskaya, U. Mohideen and V. M. Mostepanenko, Int. Ser. Monogr. Phys. **145**, 1-768 (2009) Oxford University Press, 2009
- [9] S. Wang, Y. Wang and M. Li, Phys. Rept. **696**, 1-57 (2017)
- [10] L. Vepstas, A. D. Jackson and A. S. Goldhaber, Phys. Lett. B **140**, 280-284 (1984)
- [11] M. S. Morris, K. S. Thorne and U. Yurtsever, Phys. Rev. Lett. **61**, 1446-1449 (1988)
- [12] J. Maldacena and A. Milekhin, Phys. Rev. D **103**, no.6, 066007 (2021)
- [13] P. Kovtun, D. T. Son and A. O. Starinets, Phys. Rev. Lett. **94**, 111601 (2005)
- [14] R. X. Miao, [arXiv:2412.04122 [hep-th]].
- [15] J. M. Maldacena, Int. J. Theor. Phys. **38**, 1113 (1999) [Adv. Theor. Math. Phys. **2**, 231 (1998)]
- [16] G. Policastro, D. T. Son and A. O. Starinets, Phys. Rev. Lett. **87**, 081601 (2001)
- [17] M. Brigante, H. Liu, R. C. Myers, S. Shenker and S. Yaida, Phys. Rev. D **77**, 126006 (2008)
- [18] Y. Kats and P. Petrov, JHEP **01**, 044 (2009)
- [19] M. Brigante, H. Liu, R. C. Myers, S. Shenker and S. Yaida, Phys. Rev. Lett. **100**, 191601 (2008)
- [20] M. Billò, V. Goncalves, E. Lauria and M. Meineri, JHEP **04**, 091 (2016)
- [21] R. X. Miao, JHEP **06**, 084 (2024)
- [22] G. R. Dvali, G. Gabadadze and M. Porrati, Phys. Lett. B **485**, 208-214 (2000)
- [23] T. Takayanagi, Phys. Rev. Lett. **107** (2011) 101602 [arXiv:1105.5165 [hep-th]].

- [24] R. X. Miao, JHEP **06**, 043 (2024)
- [25] R. X. Miao, JHEP **07**, 098 (2019)
- [26] M. Fujita, T. Takayanagi and E. Tonni, JHEP **11**, 043 (2011)
- [27] S. de Haro, S. N. Solodukhin and K. Skenderis, Commun. Math. Phys. **217**, 595-622 (2001)
- [28] M. Miyaji, T. Takayanagi and T. Ugajin, JHEP **06**, 023 (2021)
- [29] We thank Takayanagi for valuable comments on negative brane tension and its irrelevance to conical singularity.
- [30] K. Jensen and A. O'Bannon, Phys. Rev. Lett. **116**, no.9, 091601 (2016)
- [31] Q. L. Hu, D. Li, R. X. Miao and Y. Q. Zeng, JHEP **09**, 037 (2022)
- [32] A. Buchel, J. Escobedo, R. C. Myers, M. F. Paulos, A. Sinha and M. Smolkin, JHEP **03**, 111 (2010)
- [33] K. Sen and A. Sinha, JHEP **07**, 098 (2014)
- [34] P. Bueno, H. Casini, O. L. Andino and J. Moreno, Phys. Rev. Lett. **131**, no.17, 171601 (2023)
- [35] M. Hogervorst, S. Rychkov and B. C. van Rees, Phys. Rev. D **93**, no.12, 125025 (2016)
- [36] F. P. Toldin and M. A. Metlitski, Phys. Rev. Lett. **128**, no.21, 215701 (2022)
- [37] F. Parisen Toldin, S. Dietrich, J.Stat.Mech. 2010 P11003
- [38] M. Hasenbusch, Phys.Rev.B 82 (2010) 104425
- [39] A. Romeo and A. A. Saharian, J. Phys. A **35**, 1297-1320 (2002)
- [40] S. Bellucci and A. A. Saharian, Phys. Rev. D **80**, 105003 (2009)
- [41] M. Krech, The Casimir Effect in Critical Systems (World Scientific, London, 1994).
- [42] D. M. McAvity and H. Osborn, Nucl. Phys. B **406**, 655-680 (1993)
- [43] H. W. J. Bloete, J. L. Cardy and M. P. Nightingale, Phys. Rev. Lett. **56**, 742-745 (1986)
- [44] R. X. Miao and C. S. Chu, JHEP **1803**, 046 (2018)